Anatolian Journal of Computer Sciences

Volume:3 No:2 2018 © Anatolian Science

pp: 44-56 ISSN:2548-1304

An Expert Systems for Brain MR Images Classification by Using Ensemble Neural Network

Ali ARI[1*], *Davut HANBAY*[2],

[*1]*Department of Computer Eng.,Inonu University,Malatya,Turkey (ali.ari@inonu.edu.tr)*

[2]*Department of Computer Eng.,Inonu University, Malatya,Turkey (davut.hanbay@inonu.edu.tr)*

Received:14.08.2018

Published: Sep, 2018

Abstract—

Magnetic Resonance Imaging (MRI) is a useful technique for diagnosis of abnormalities that may occur in brain and other tissues. Detection of brain tumors in MRI is a difficult task for physicians. Because they must consider the textural, statistical, morphological and color features of the MR images at the same time to determine the tumors. In this paper, a robust brain MR images classifier based on hybrid features by using Ensemble Neural Network (ENN) is proposed. To increase the robustness of the classifier textural, statistical and color features were used as input to the ENN model. The main advantage of proposed method is reducing image dimension and using ensemble neural networks method to increase accuracy. This ensemble based method combines the base classifiers predictions to increase the proposed model performance and evaluated accuracy and AUC values are 98.70 %, 0.976, respectively. These results were compared with the other methods in literature.

Keywords : *Brain MRI, Ensemble Neural Network, Feature extraction, 2D Wavelet Transform*

1. Introduction

The brain is the most complex organ that acts as a central nerve system. All functions of the body are controlled by the brain. Brain tumor can affect the normal functionality of brain. It is one of the most common causes of the mortality in the world. The early diagnosis of tumor is beneficial for successful treatment. A vast number of benign brain tumors are known as noncancerous. They are not harmful at all and they do not tend to expand to nearby tissues, even though in certain incidents benign tumors could be critical. We certainly know that malignant brain tumors are basically abnormal brain cells that leads to cancer and it is known that these tumors grow faster than benign tumors by spreading to neighboring tissues around the area. MRI is one of the imaging techniques for analyzing and researching the behavior of the body parts. MRI studies have become popular in recent years. By reason of it is a non-invasive procedure that presents the soft tissues with high resolution and produces multiple images of the same tissue with different contrast [1]. So, it provides useful information for physicians about human soft tissues anatomy. Manual detection of tumors in MRI requires trained radiologists. However, this is a time consuming process to [2]. Manual detection, recognition and segmentation of such a big data is useless because of the fact that number of patients and their images are voluminous [2]. Henceforth; we require to automate this process based on segmentation techniques. The increased interest in medical imaging has gained importance from the need for automated and influential diagnosis in a brief time. There are a lot of techniques based on image processing and artificial intelligence which have been applied for early detection of brain tumor. Brain MRI is segmented in two parts. One part represents normal brain cells while the other

one represents tumorous brain cells. The accuracy of the segmentation is very crucial. Usually MR images are barely highly contrast that means these segments can be easily overlapped with each other [3]. In order to locate the brain structures, three principal planes are used: The axial plane divides the brain into cranial and caudal (head and tail) portions. The coronal plane divides the brain into dorsal and ventral (back and front) portions. The sagittal plane is a plane parallel to the sagittal suture. It divides the brain into left and right hemisphere [4]. These 3 planes are shown (see Figure 1).

Figure 1. Exemplary MR images, (a).axial plane, (b).coronal plane, (c).sagittal plane

There are some studies on brain images analysis. In [1] it is shown that two different sets of texture-based feature extraction techniques were applied. The first one was the Gabor wavelet feature. The second set was statistical based texture features which were Gray Level Co-Occurrence Matrix (GLCM), Gray Level Run Length Matrix (GLRLM), Histogram of Oriented Gradient (HOG), and Local Binary Pattern (LBP). Several classifiers such as Support Vector Machine (SVM), K-Nearest Neighbor (KNN), Sparse Representation Classifier (SRC), Nearest Subspace Classifier (NSC), and K-Means clustering were used in simulations [1]. In [5], GLCM and law's energy were used for feature extracting from wavelet transform of MR images. Tumor classification process was performed via ANFIS. In [6], a discrete wavelet based genetic algorithm method was presented to detect the tumor in brain MR images. At first, MR images were enhanced using discrete wavelet descriptor, and then genetic algorithm was applied to detect the tumor pixels. The efficiency of genetic algorithms and unsupervised image segmentation was demonstrated. In [7], it was laid out that the ensemble SVM was used for classification. Genetic Algorithm was applied for optimizing the weights. Finally, FCM clustering method was used to extract tumor portion from this obtained brain portion. In [8], Histogram-Based Gravitational Optimization Algorithm (HGOA) method was used. The proposed method was fully automatic. They also upgraded the level of the gravitational optimization algorithm. In [9], each MR images in the training set was pre-processed to minimize the intensity bias and to remove the non-brain tissue. Following that; intensity, symmetry, shape deformation and texture features were extracted. AdaBoost was used to perform feature selection and fusion. In [10], edge detection operation watershed method was used which was a color based algorithm using HSV color space in its structure. Then contrast enhancement watershed algorithm was applied for each region. A detector which identifies Canny edge was applied to output image. Combining these three segmented images provided that brain tumor was determined. The algorithm was tested on twenty brain MR images. The proposed algorithm offered encouraging results. In [11], a hybrid technique for brain tumor detection and classification through MRI was proposed. Firstly, image preprocessing which includes noise filtering, skull detection was applied. Secondly, feature extraction from brain MR images using GLCM was applied. Thirdly, classification of inputs into normal or abnormal using Least Squares Support Vector Machine classifier with Multilayer perceptron kernel was performed. In [12], a method for the brain tumor detection and segmentation was proposed. In first stage symmetry analysis of grey levels was utilized to detect the existence of tumor. In second stage, segmentation was carried out based on edge detection. Presented edge detection method was based on F-transform model which captures the silent edges. After edge detection, a morphological operation was adopted for the final stage to obtain only tumor.

In this study, a decision support system was presented for detecting tumor from brain MR images and classifying whether they are benign or malignant tumors. Proposed system is composed of five stages; these are two dimensional wavelet transform, preprocessing, segmentation, feature extraction and classification. At first, Brain MR images were divided into 4 sub bands by applying two

dimensional wavelet transform. Instead of original image, the approach coefficient sub band which was 4 times smaller than the original image was used. After that, median filter is applied to the brain MR images to remove the noise. Location of tumors has been defined by applying Otsu Method and with the help of appropriate threshold value. Statistical, color and textural based features were extracted from detected tumor. These features were combined to obtain robust classifier. ANN models were used for each brain structure (axial, coronal, sagittal) and to evaluate the outputs. Proposed model performance was measured by accuracy and AUC criteria. These are 98.70 %, 0.976 respectively.

The paper is organized as follows: Section 2 introduces the preprocessing method that contains image enhancement and tumor segmentation. Section 3 introduces the feature extraction process. Artificial Neural Networks are explained in Section 4. Results are presented in Section 5. In Section 6, the conclusion of this work is stated.

2. Materials and Methods

2.1. Two Dimensional Wavelet Transformation

Wavelet transform is preferred in order to obtain time-frequency representation of a signal or image [13,14]. Wavelet transform has been used to make further detailed researches on the images whose background and foreground are closer such as brain MR image. Also this technique has been applied in many fields [15]. In this study, MR images was divided into 4 sub-band. This transform is shown in (see Figure 2). Here A: approaching coefficients of sub-band image, H: horizontal coefficients of sub-band image, V: vertical coefficients of sub-band image, D: diagonal coefficients of sub-band image.

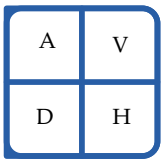

Figure 2. Single layer decomposition of two dimensional wavelet transform.

General wavelet transform formula is provided in Equation 1 and Equation 2 [16].

$$WT(a,b) = \frac{1}{\sqrt{a}} * \int x(t) * \psi * (\frac{1}{a}) dt \quad (1)$$

$$x(t) = \frac{C_\psi}{a^2} * \int_{a>0} \int_b WT(a,b) * \psi * (\frac{t-b}{a}) da\ db. \quad (2)$$

In Equation 2: where a : scaling parameter (a >0), b : dilation parameter, ψ : main wavelet, C_ψ is wavelet depended constant, $\psi(a,b)$ is the wavelet family.

2.2. Image preprocessing

Images can be effected from noises. The aim of the image preprocessing was to remove those noises from MR images to increase the system accuracy. Image preprocessing steps used in this study are given in following steps.

Image filtering: The median filter is a nonlinear digital filtering technique, often used to reduce the noise in an image. It is a typical preprocessing in digital image processing such as edge detection. Median filter is used for removing digitized noise from signal or image without descending of image sharpness.

The morphology and segmentation with the method of Otsu: The Otsu method is a threshold detection method which can be applied to gray level images [17]. When this method is used, it's

assumed that images are formed from two color ranges called background and foreground [17]. Afterwards, for all the threshold values, the range of variance values of these two color ranges is calculated. The threshold value which makes this value the minimum value is the optimal threshold value. The most morphological processes are adding the pixels to the edges of the objects (opening) and removing the pixels from the edges of the objects (closing). Applying Otsu threshold to the image, after purely black and white image is obtained, unwanted components like tags are removed from the image with the morphological opening and closing processes.

Image enhancement: Histogram equalization is the most common method used to improve the low visibility of an image [18]. Transforming the input histogram into a histogram having equal pixel number in each gray level, it makes the output histogram have uniform distribution. Histogram equalization can be expressed as in the Equation 3 [18].

$$s_k = \sum_{j=0}^{k} \frac{n_j}{n} * (L-1), \qquad k = 0,1,2,...,L-1 \tag{3}$$

Where, $\boldsymbol{n}$ is total number of pixel in input image,$\boldsymbol{n_j}$ is the pixel number at gray level of $\boldsymbol{j}$. $\boldsymbol{L}$ is possible total gray level number, $\boldsymbol{s_k}$ is gray level transition value for having better contrast image.

3. Feature Extraction

Features such as the shapes, positions, dimensions and densities of the mass as a result of the segmentation process of the MR images must be detected. Therefore, Features belongs to shape, textural, color and wavelet transform of the mass are obtained at this stage.

3.1. Statistical Features

Mean, variance, skewness and kurtosis features are generally used for obtaining characteristic of images [19].

Mean is the moderate value of the density of the image.

$$\mu = \sum_{i=0}^{N-1} iP(i) \quad , \qquad \boldsymbol{N} \text{ denotes number of samples} \tag{4}$$

Variance measures the density gradient around the average.

$$\sigma^2 = \sum_{i=0}^{N-1} (1-\mu)^2 P(i) \tag{5}$$

Skewness, a central point on the image is selected and if the image is the same on the left and on the right of the point, it is understood that the data is symmetric. If the measure of asymmetry is a value smaller than zero, it means the histogram is skewed to the left, if it is bigger than zero; it is skewed to the right.

$$\sigma^{-3} \sum_{i=0}^{N-1} (i-\mu)^3 P(i) \tag{6}$$

Kurtosis concept is the measurement of the features of the sharpness or kurtosis resulting from the defined graphical representation of the probability distribution for the real-valued variable.

$$\sigma^{-4} \sum_{i=0}^{N-1} (i-\mu)^4 P(i) - 3 \tag{7}$$

3.2. Gray Level Thresholding

It is believed that level of white spots on MR image is effective on cancer. When this value increases, the possibility of being malignant increases too. Therefore, gray thresholding level belonging to the image is used as feature [20].

3.3. Local Binary Pattern

LBP is a texture analysis operator. It is a texture measurement method which is independent of gray level. Original LBP operator creates a tag for each pixel of the image [21]. This tag is a binary number obtained as a result of the comparison of the central pixels to the 3x3 pixel neighborhood. Each image pixel is tagged as the difference between its neighbors and itself is doubled with $u(x)$ step function [22].

$$LBP_{P,R}(x_C) = u(x_p - x_c)2^p,\ u(y) = \begin{cases} 1, & y \geq 0 \\ 0, & y < 0 \end{cases} \quad (8)$$

Where, x_c represents the LBP tag production center pixel, x_p represents the neighbors of the center pixel, R represents the neighbors' distance to the center and P represents the number of processed neighbors. (See Figure 3) the implementation of the LBP operator is demonstrated.

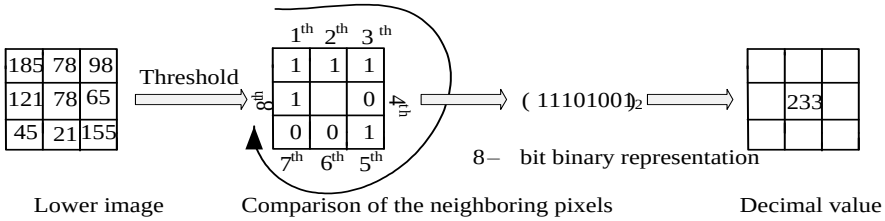

Figure 3. The implementation of the LBP operator.

It's observed in the conducted studies that the majority of the texture surfaces of the images are uniform patterns. Uniform patterns are 0-1 or 1-0 in binary LBP code whose transition number is fewer than 2. For example, as 00000000 and 11111111 patterns have 0 transition and 01100000 and 11000011 patterns have 2 transitions, they are uniform patterns [22]. Uniform patterns can explain the simple textures such as spot, edge and corner. There are a total of $Px(P-1)+2$ uniform patterns. As the values of non-uniform pixels are kept to 1 histogram, the LBP histogram will have 59 bins. The presentation of the LBP uniform histogram shown in (see Figure 4).

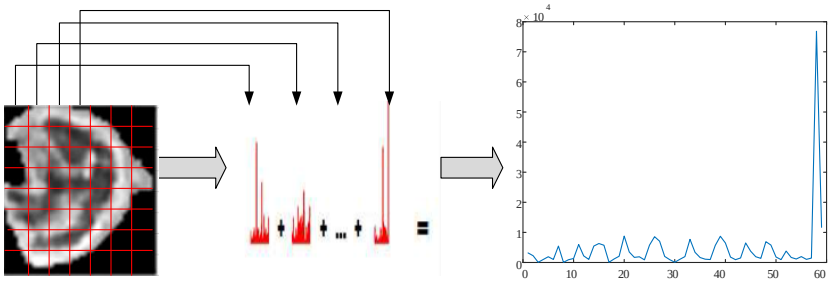

Figure 4. The Presentation of the LBP Uniform Histogram

3.4. Gray Level Co-Occurrence Matrix

Gray Level Co-Occurrence Matrix (GLCM) is a feature extraction method comparing the gray level differences between the two different pixels of the pattern identified by Haralick [23]. The first pixel is known as the reference while the second pixel is known as the neighbor pixel [24]. Being P(I,j|d,0), this matrix is formed with the angular relation between the pixels in the sub band image and the function of the distance. While the distance between pixels is d, the angle is 0, P(I,j) shows the transition probability from gray level I to gray level j. With the range of 45° angles, four matrices are obtained for each distance. P(0,d), P(45,d), P(90,d), P(135,d) the directions of the 45° angles are demonstrated around the selected pixel in (see Figure 5).

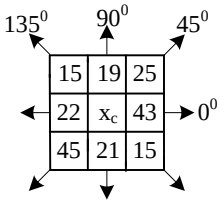

Figure 5. The presentation of the angles for the selected pixel.

Contrast: It is the measurement of the density or gray level variations between the reference pixel and its neighbors [25]. In the Equation 9 i and j show the row and column indices.

$$\sum_{i,j} |i-j|^2 P(i,j) \tag{9}$$

Correlation: It measures the linear dependence of the gray level values in the co-occurrence matrix. Besides, it demonstrates in what way it is in relation to its neighbor in the reference pixel [25]. In the correlation equation observed in the Equation 10. P shows the GLCM component, σ shows the standard deviation while μ demonstrates the average.

$$\frac{\sum_{i,j}(ij)P(i,j)-\mu_x\mu_y}{\sigma_x\sigma_y} \tag{10}$$

Energy: It returns the sum of squared elements in the GLCM. Uniformity, uniformity of energy, and angular second moment which are known as the properties of energy [25]. The formula of energy is as in following Equation 11.

$$\sum_{i,j} P(i,j)^2 \tag{11}$$

Homogeneity: It is the measure of the similarity of different sections of the image [25]. The formula of homogeneity is given in Equation 12.

$$\sum_{i,j} \frac{P(i,j)}{1+|i-j|} \tag{12}$$

Entropy: Entropy is defined as randomness and irregularity. It expresses how often the patterns repeat for this study [25]. The formula of entropy is given in Equation 13.

$$-\sum_{i,j}^{N} P(i,j) * \log P(i,j) \tag{13}$$

The reverse of the normalized momentum difference: A measure of the local homogeneity of an image [25]. The Formula calculating the reverse of normalized momentum difference is given in Equation 14.

$$\sum_{i,j}^{N} \frac{1}{1+(i-j)^2} P(i,j) \tag{14}$$

3.5. Wavelet Energy

Energy value of attributes vector belonging to the coefficient of image in different scales by wavelet transform was calculated. At a certain scale energy distribution change parameter referenced method at texture analysis because of contains important information. The energy of the channel output is given Equation 15 [26]. In formula N is block height in pixel and M is block width in pixel.

$$E_{ni} = \frac{1}{NM} \sum_{j}^{N-1} \sum_{k}^{M-1} D_{ni}(b_j, b_k)^2 \tag{15}$$

4. Artificial Neural Networks (ANNs)

ANNs consisting of many neurons are biologically infused and characterize the human brain. ANNs model is shown in (see Figure 6). Each weight has a particular value that multiplied by transferred signal in network. Every neuron output is determined by its activation function. Many type of activation function are used in literature. Mostly, activation functions such as tangent sigmoid, etc. are used [27]. ANNs have generalization ability; so they can product an output as implemented an unknown input to the studied network [28-30]. The neuron output can be evaluated by Equation 16.

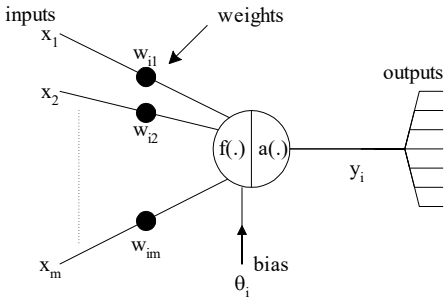

Figure 6. The structure of ANNs model [29].

$$y(t+1) = a\left(\sum_{j=1}^{m} w_{ij}\, x_j(t) - \theta_i\right),\ f_i \triangleq net_i = \sum_{j=1}^{m} w_{ij}\, x_j - \theta_i \qquad (16)$$

Where, x= (xX1, xX2,…, xXm) exhibited the m inputs parameters of the neuron, w_i represents the weights for input (x_i,θ_i)is represents the bias value, a(.) represents the activation function. ANNs have been employed for data mining, communications, modeling of nonlinear systems, medical applications and pattern matching by means of their parallel processing capabilities. When designing ANNs model, a number of parameters must be considered. First of all, the convenient type of the ANNs model must be determined, thereafter appropriate activation function need to be determined. The number of neuron in each layer must be selected. They can be easily modeled by high-capacity computers [31-32].

5. Application

The proposed method is detailed in this section. The data used in this study was taken from [33]. All images are in DICOM file format. All images used in the data set were digitized at 256x256 pixel and 16-bit in gray levels. 16 patients' data were used in this study. 140 benign tumors, 140 malignant tumor images belonging to axial, coronal and sagittal plane. 9 patients' images were used for training and the rest is used for testing. Partitioning is done in a patient wise manner. All Program codes were written in MATLAB with the computer 3.50 GHz CPU and 8 GB RAM. The block diagram of the proposed model is shown in (see Figure 7).

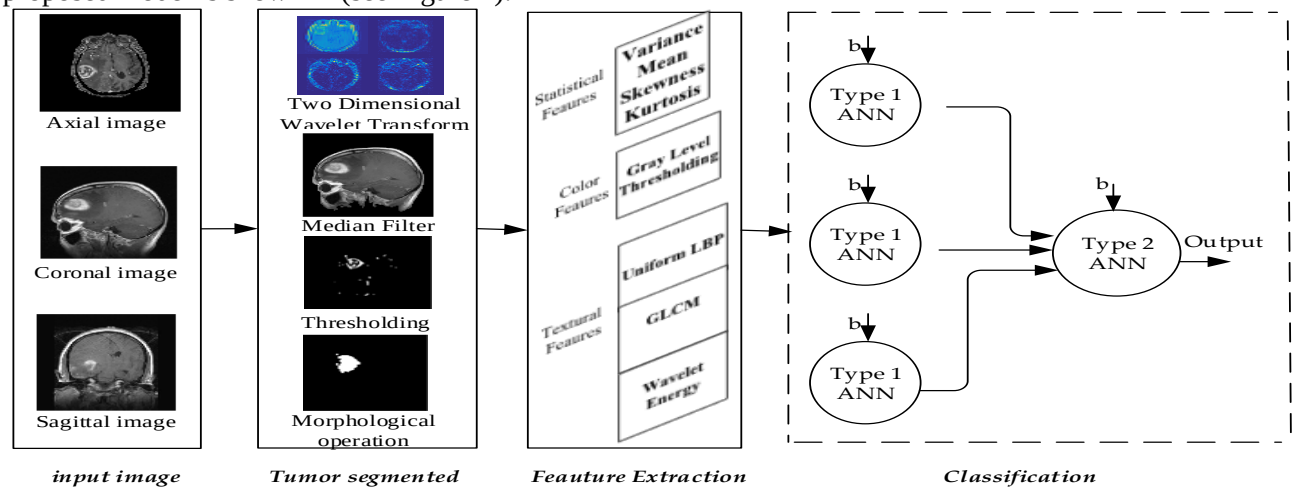

Figure 7. Block diagram of the proposed model.

Firstly, the images taken from the database were transformed to 4 sub-band applying 2 level discrete wavelet transform with symlet wavelet. Instead of original image, the image approximation sub bands were used. So the size of the images was reduced. Process steps are shown in (see Figure 8).

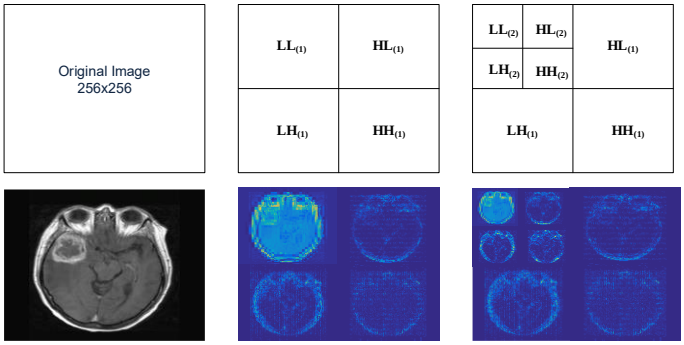

Figure 8. Wavelet transformation applied images.

Afterward, all images are preprocessed by Median filter. This process step is shown in (see Figure 9).

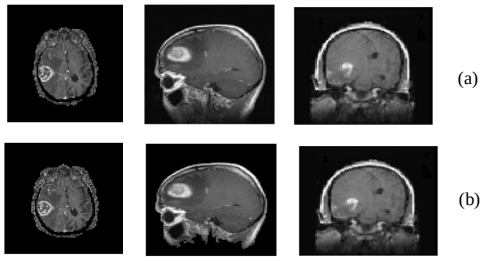

Figure 9. (a). Original MR images, (b) preprocess applied image.

After preprocessing thresholding, opening, closing and edge detecting process were applied to determine the interested region on MR images. The images obtained after this process are shown in (see Figure 10).

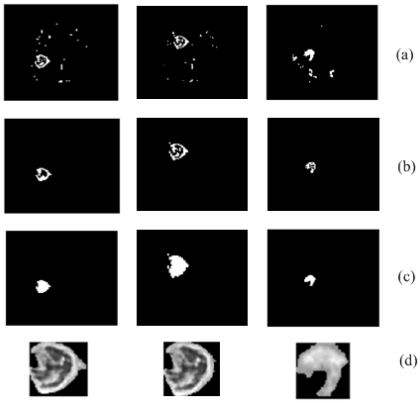

Figure 10. (a). Thresholding image, (b). opening process, (c). closing process, (d). tumor detection

Statistical, gray level thresholding, LBP, GLCM and wavelet Energy based features are combined to have robust brain tumor detecting system. There are four statistical features. these are mean, variance, skewness and kurtosis. There is also one gray level threshold value. 59 features of uniform LBP were obtained using P=8 and R=1. The used GLCM features were Contrast, Correlation, Energy, Homogeneity, Entropy and the reverse of the normalized momentum difference. GLCM features were extracted from $h = 0^\circ, 45^0, 90^\circ, 135^0$ rotated images. In each rotation, GLCM matrix

and six features were calculated. Addition to these features, 7 features from wavelet energy were used. Totally 95 attributes have been extracted from each image.

Table 1. Type 1 ANN model architecture and training parameters

Architecture	
The number of layers	3
The number of neuron on the layers	Input: 95, Hidden: 10, Output : 1
The initial weights and biases	Random
Activation Functions	Tangent-sigmoid ,Tangent-sigmoid, Linear
Training parameters	
Learning rule	Scaled Conjugate Gradient
Sum-squared error	0.0000001

ANN is used for classification. Two types ANN models were used type 1 for each spatial space and the type 2 for to combine these models outputs. The properties of Type-1 ANN model for spatial space is given in (see Table 1). It has 3 layer, 95 inputs, 2 outputs, the number of neuron in the hidden layer is 10. Quality parameters are used to analyze the proposed technique. It is including sensitivity, accuracy, and positive predictive value (PPV).

$$Sensitivity = \frac{(TP)}{(TP + FN)} \tag{17}$$

$$Accuracy = \frac{(TP + TN)}{(TP + FN + TN + FP)} \tag{18}$$

$$PPV = \frac{TP}{(TP + FP)} \tag{19}$$

The accuracy evaluated by using MR images which contains tumors. P means Malignant tumor. N means benign tumors. Where TP is the number of true-positives, TN is the number of true negative, FP is number of false-positives and FN denotes the number of false-negatives. Type 1 ANN models outputs' accuracy, sensitivity, positive predictive value is given in (see Table 2).

Table 2. Evaluated Success parameters of each spatial plane's designed system

Spatial plane	Accuracy	Sensivity	Positive Predictive Value
Axial	%97.50	%97.84	%97.14
Coronal	%98.21	%98.56	%97.85
Sagittal	%97.14	%97.82	%97.13
Mean	%97.61	%98.07	%97.37

There are some existing studies in literature they suggested several methods. These methods were applied to the same dataset by us. In [1], the Gabor-wavelet features are extracted by applying Gabor-wavelet kernels with five different scales and eight orientations on three different window sizes as 33x33, 45x45, and 65x65.

In [5], GLCM, wavelet and law's energy texture features were used. Four GLCM features were extracted from $h = 0^{\circ}, 45^{0}, 90^{\circ}, 135^{0}$ each rotated images. Used GLCM features which are Contrast,

Energy, Homogeneity Correlation. Totally 16 features were used. For the comparison of the existing methods and proposed method, different type classifiers such as SVM, KNN and ANN were used. These methods performance were compared with the proposed method and tabulated in (see Table 3).

Table 3. Comparison of various classifiers on Gabor-wavelet and statistical features

Methodology	**SVM Linear**			**KNN(k=7)**			**ANN**		
	Axial	**Coronal**	**Sagittal**	**Axial**	**Coronal**	**Sagittal**	**Axial**	**Coronal**	**Sagittal**
[1]	%92.43	%94.50	%92.12	%96.50	%94.13	%95.42	%96.83	%97.15	%96.26
[5]	%96.13	%95.20	%91.42	%97.25	%97.43	%96.59	%96.30	%95.20	%94.31
Prop. Method	**%96.85**	**%96.11**	**%91.12**	**%97.85**	**%98.26**	**%96.83**	**%97.50**	**%98.21**	**%97.14**

The properties of Type-2 ANN model are given in (see Table 4). It has 3 layer, 6 inputs, 2 outputs, the number of neuron in the hidden layer is 5.

Table 4. Type 2 ANN model architecture and training parameters

Architecture	
The number of layers	3
The number of neuron on the layers	Input : 6 Hidden : 5 Output : 1
The initial weights and biases	Random
Activation Functions	Tangent-sigmoid Tangent-sigmoid Linear
Training parameters	
Learning rule	Scaled Conjugate Gradient
Sum-squared error	0.0000001

The proposed ensemble model training performance is shown in (see Figure 11).

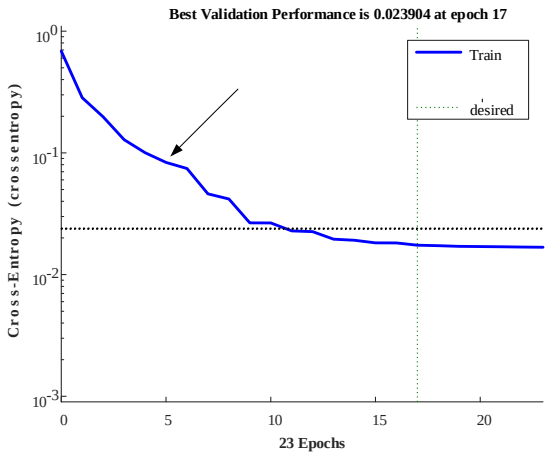

Figure 11. Training performance

The performance of the ensemble model is determined by AUC and ROC. Evaluated AUC value is 0.976 and ROC of the ENN model is shown in (see Figure 12).

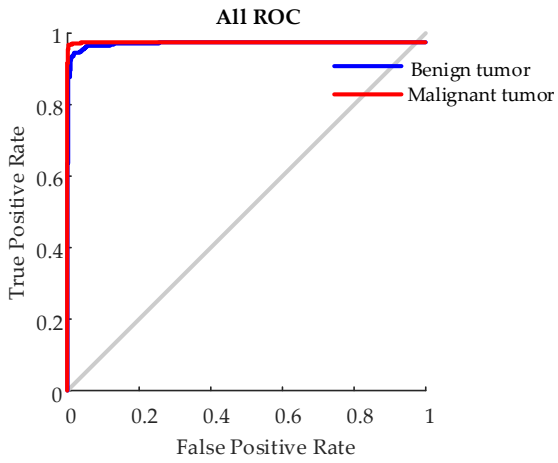

Figure 12. Roc graph of Type 2 ANN model

The outputs of each type 1 ANN models were (malignant and benign) applied to Type 2 ANN model. Type 2 ANN model has 6 inputs and 2 output (malignant and benign). Overall system accuracy was increased to 98.70 %. Ensemble method is increased the system's performance.

6. Conclusion

In this study, an ensemble ANN model was presented for brain tumor segmentation and classification based on hybrid features extracted from MR images. Detected tumors were classified as benign or malignant. The axial, coronal and sagittal plane MR images were used. The image size in each plane was 256x256. Using each plane images to detect tumor improves the accuracy and at the same time it increases the computation complexity. To overcome this problem MR images dimension were reduced from 256x256 to 64x64 by using 2D wavelet transform. Obtaining a more accurate system we have to use efficient features extracted from images. These features can be based on color, texture and statistic. Combining these features can increase the models performance. Therefore, these three kind of features were used in proposed system. Different classifier can be used to classify these features. But classifier accuracy depends on the features and classifier types. ANN is one of the well-known classifier in such studies. For improving ANN model accuracy ensemble method was applied. Two type ANN model were used to construct the ensemble model. Type 1 was used for classifying each plane images and type 2 was used to classify each plane ANN models outputs. To evaluate the suggested system performance a dataset was used that is available publicly. Two performance measures such as area under the curve and accuracy were used. Evaluated accuracy and AUC values are 98.70 %, 0.976 respectively. The suggested methodology can be used to increase tumor detection and classification tasks. This model can be used in examining the brain tumors.

Funding:

This study was not funded by any organization

Conflict of Interest:

The authors declare that they have no conflict of interest.

Data Availability:

The data used in this study can be accessed at http://brainweb.bic.mni.mcgill.ca/brainweb

References

[1] Nabizadeh N, Kubat M (2015) Brain tumors detection and segmentation in MR images: Gabor wavelet vs. statistical features. Computers & Electrical Engineering vol. 45: 286–301.

[2] Aslam A, Khan E, Beg MMS (2015) Improved Edge Detection Algorithm for Brain Tumor Segmentation. Procedia Computer Science Volume vol.58, pp.430–437.

[3] Ain T-S, Jaffar Q, Choi MA (2014) Fuzzy anisotropic diffusion based segmentation and texture based ensemble classification of brain tumor. Applied Soft Computing vol.21, pp.330–340.

[4] Available Online (2016) https://en.wikipedia.org/wiki/Anatomical_. Accesed 16 October 2016.

[5] Shanthakumar P and Ganeshkumar P (2015) Performance analysis of classifier for brain tumor detection and diagnosis. Computers & Electrical Engineering vol.45, pp.302–311.

[6] Chandra GR., Rao KRH (2016) Tumor Detection In Brain Using Genetic Algorithm. Procedia Computer Science vol.79, pp.449–457.

[7] Ain Q, Jaffar MA, Choi TS (2014) Fuzzy anisotropic diffusion based segmentation and texture based ensemble classification of brain tumor. Applied Soft Computing vol.21, pp.330–340.

[8] Nabizadeh N, John N, Wright C (2014) Histogram-based gravitational optimization algorithm on single MR modality for automatic brain lesion detection and segmentation. Expert Systems with Applications vol.41, pp.7820–7836.

[9] Ghanavati S, Li J, Liu T, Babyn PS, Doda W, Lampropoulos G.(2012) Automatic brain tumor detection in Magnetic Resonance Images. 9th IEEE International Symposium, Barcelona, Spain.

[10] Maiti I, Chakraborty M. (2012) A new method for brain tumor segmentation based on watershed and edge detection algorithms in HSV colour model. Computing and Communication Systems (NCCCS), 2012 National Conference on, Durgapur, India.

[11] Praveen GB, Agrawal A (2014) Hybrid approach for brain tumor detection and classification in magnetic resonance images. 2015 International Conference on Communication, Control and Intelligent Systems (CCIS), Tehran, Iran.

[12] Al-Azzawi NA, Sabir MK (2015) An superior achievement of brain tumor detection using segmentation based on F-transform. Computer Networks and Information Security (WSCNIS), Hammamet, Tunisia.

[13] Araújo MC, Lima RCF, De Souza RMCR (2014) Interval symbolic feature extraction for thermography breast cancer detection. Expert Systems with Applications vol. 41, pp.6728–6737.

[14] Pereira DCR, Ramos P, Nascimento MZ (2014) Segmentation and detection of breast cancer in mammograms combining wavelet analysis and genetic algorithm.Computer Methods and Programs in Biomedicine vol: 114, pp.88–101.

[15] Mohanalin J, Beena mol M (2014) A new wavelet algorithm to enhance and detect microcalcifications. Signal Processing vol. 105, pp.438–448.

[16] Alpaslan N, Imik O, Hanbay D (2016) Breast Mass Classification in Mammogram Images Based on Wavelet Transform. International Conference on Natural Science and Engineering (ICNASE'16), Kilis, Turkey.

[17] Zhang X, Zhao H, Li X, et al. (2016) A multi-scale 3D otsu thresholding algorithm for medical image segmentation. Digital Signal Processing vol.60, pp.186–199.

[18] Zahedi M, Rahimi M (2016) 3-D color histogram equalization by principal component analysis. Journal of Visual Communication and Image Representation vol.39, pp.58–64.

[19] Ari A, Hanbay D (2016) Detection of Brain Tumor from the MR Images by Using Hybrid Features. International Conference on Natural Science and Engineering (ICNASE'16) , Kilis, Turkey.

[20] Ari A, Alpaslan N, Hanbay D (2015) Computer-aided tumor detection system using brain MR images. Tıp Teknolojileri Ulusal Kongresi (TIPTEKNO'15), Bodrum, Turkey.
[21] Zhao C, Qiao S Sun J, et al. (2016) Sparsity-based shrinkage approach for practicability improvement of H-LBP-based edge extraction. Nuclear Instruments and Methods in Physics Research Section A: Accelerators, Spectrometers, Detectors and Associated Equipment vol. 825, pp.1–5.
[22] Kaya Y, Ertugrul OF, Tekin R (2015) Two novel local binary pattern descriptors for texture analysis. Applied Soft Computing vol.34, pp.728–735.
[23] Sengur A, Guo Y, Akbulut Y (2016) Time–frequency texture descriptors of EEG signals for efficient detection of epileptic seizure. Brain Informatics, vol.3, pp.101–108.
[24] Arabi PM, Joshi G, Vamsha Deepa G (2016) Performance evaluation of GLCM and pixel intensity matrix for skin texture analysis. Perspectives in Science, vol.8, pp.203–206.
[25] Malegori C, Franzetti L, Guidetti R et al., (2016) GLCM, an image analysis technique for early detection of biofilm. Journal of Food Engineering, vol:185, pp.48–55.
[26] García M, Ródenas J, R.Alcaraz, et al. (2016) Application of the relative wavelet energy to heart rate independent detection of atrial fibrillation. Comput Methods Programs Biomed, vol.131, pp.157–168.
[27] Colak MC, Colak C, Kocaturk H, et al., (2008) Predicting coronary artery disease using different artificial neural network models. Anatol. J. Cardiol. vol.8, pp.249–255.
[28] Marshall JA (1995) Neural networks for pattern recognition. Neural Networks, vol.8, pp.493–494.
[29] Hanbay D, Turkoglu I, Demir Y (2010) Modeling switched circuits based on wavelet decomposition and neural networks. Journal of the Franklin Institute, vol.347, pp. 607–617.
[30] Suykens JAK, Vandewalle J (1999) Least Squares Support Vector Machine Classifiers", Neural Processing Letters, vol.9, pp.293–300,
[31] Firat F, Arslan AK, Colak C, et al., (2016) Estimation of risk factors associated with colorectal cancer. an application of knowledge discovery in databases. Kuwait Journal of Science, vol.43, pp.151–161.
[32] Rafiq MY, Bugmann G, Easterbrook DJ (2001) Neural network design for engineering applications. Computers & Structures. vol.79, pp.1541–1552.
[33] BrainWeb: Simulated Brain Databases (2017) http://brainweb.bic.mni.mcgill.ca/brainweb. Accessed 17 May 2017.